

Synchronous Update and Optimization Method for Large-Scale Image 3D Reconstruction Technology Under Cloud-Edge Fusion Architecture

Jian Zhang^{1*}, Jingbin Luo², Yilong Chen³

Guangdong Power Grid Co., Ltd, Guangzhou 510030, China^{1, 2}

Guangdong Power Grid Co., Ltd, Guangzhou Power Supply Bureau, Guangzhou 510000, China³

Abstract—Aiming at the problems of limited bandwidth and network delay in the traditional centralized cloud computing mode during large-scale image processing of transmission and distribution digital corridors, a synchronous updating and optimization method for large-scale image 3D reconstruction technology under cloud-edge fusion architecture is proposed. Based on the cloud-side fusion architecture, the image data of the transmission and distribution corridor is preprocessed, feature extraction is performed by deep learning, synchronous updating is performed by using the cloud-side cooperative network, and matching and 3D reconstruction are performed according to the order of the point cloud data; given the dynamically changing characteristics of the image data in the cloud-side fusion environment, the incremental learning is combined with the continuous learning and synchronous updating of the model parameters, to realize the adaptive updating mechanism. The research method utilizes the advantage of cloud-edge fusion architecture to distribute the computational tasks to the cloud and edge, realizing parallel processing and load balancing, and improving the accuracy and efficiency of 3D reconstruction. The experimental results show that the research method in this paper has an image feature point matching rate as high as 96.72%, a lower network latency rate, and a higher real-time performance, which provides strong technical support for the optimization of the transmission and distribution digital corridor 3D reconstruction technology.

Keywords—Cloud-edge fusion; cloud-edge collaboration; 3D reconstruction; synchronized update

I. INTRODUCTION

With the in-depth promotion of intelligent transformation in the power industry, 3D reconstruction technology is widely used in the construction of digital corridor models, and the study of 3D reconstruction technology with efficient synchronization performance is of great significance to enhance the construction and management efficiency of transmission and distribution corridors. The study in [1] designed a point cloud data extraction process based on tilt photography technology, combined with the optical distortion problem for 3D modeling of transmission lines, which can quickly obtain the target shape, but the throughput of remote image communication is not high and the transmission rate is low. The study in [2] fuses transmission line channel information based on visible image sequences, sets the model

geometry through standardized mapping space, establishes mapping relationship with power line point cloud data and images, and constructs 3D reconstruction model under the constraint relationship function, but the technique lacks double-ended synchronous communication system and centralized network information processing efficiency is not high. The research in [3] introduces the cloud-side cooperative function to realize the global resource sensing and cooperative scheduling of star-earth fusion network, and combines the arithmetic network technology to provide a new technical path for the synchronous transmission of large-scale image 3D reconstruction. The study in [4], on the other hand, provides a comprehensive overview of the development history of image 3D reconstruction technology, evaluation methods and datasets. Image 3D reconstruction techniques have made remarkable progress, from early geometric model-based methods to today's advanced algorithms based on deep learning, the accuracy and efficiency of reconstruction have been continuously improved. However, current 3D reconstruction techniques still face many challenges. On the one hand, the synchronized processing of large-scale image data puts forward extremely high requirements on computational resources and storage capacity, which are often difficult to be met by traditional centralized architectures. On the other hand, images from different data sources differ in quality, angle, illumination, etc., how to effectively fuse these images for accurate 3D reconstruction is still a difficult problem. Therefore, this paper provides new ideas and methods to solve the difficulties in large-scale image 3D reconstruction. By fully utilizing the advantages of cloud-edge fusion architecture, it can effectively integrate computational resources, improve reconstruction efficiency and accuracy, and meet the urgent needs of image 3D reconstruction in different fields. Innovative use of cloud computing and edge computing technology for organic combination, cloud-edge cooperative network can effectively improve the double-end communication throughput, providing powerful technical support for large-scale image 3D reconstruction. At the same time, the 3D reconstruction algorithm is optimized and improved by combining deep learning to improve the reconstruction accuracy and efficiency, providing a more efficient technical path and solution for the 3D reconstruction of transmission and distribution corridors, which improves the efficiency accuracy and enhances the robustness of large-scale image reconstruction from the technical level.

*Corresponding Author.

II. TRANSMISSION AND DISTRIBUTION DIGITAL CORRIDOR IOT CLOUD EDGE CONVERGENCE ARCHITECTURE

A. Cloud-edge Fusion Network Architecture

The transmission and distribution of digital corridor image 3D reconstruction system mainly adopts the cloud-edge fusion system architecture, including three key components: cloud center, edge domain, and edge nodes (see Fig. 1).

Cloud Center. The cloud center is the core of the whole architecture, responsible for processing and fusion of multi-dimensional data of the system, which can support massive 3D reconstruction image and data storage as well as synchronous data-parallel update. The cloud center aggregates the edge nodes and resource pools through the high-speed network and provides big data applications for the system through deep learning and association algorithms [5].

Edge domain. The edge domain is the "bridge" connecting the cloud center and edge nodes, with the function of data processing and forwarding. It is deployed in each key position of the transmission and distribution corridor according to the actual needs, and acquires real-time corridor information by collecting sensor data, video streams, etc., extracts key features and information through preliminary pre-processing, and then transmits them to the cloud center to realize "data in the cloud" [6].

Edge node. Edge nodes are multi-dimensional sensing front-end devices deployed at the site of transmission and

distribution corridor, with the ability to data acquisition, processing, and execution of control commands. The front-end node acquires the image, temperature, humidity, and other environmental information of the corridor in real time, adjusts the parameters of the equipment to carry out special operations, and sends the front-end information to the cloud center through the convergence of the edge domain.

B. Cloud Data Center Structure Optimization

Large-scale image three-dimensional reconstruction technology requires parallel processing of massive data, the cloud data center should take large-capacity, high-speed, and stable equipment to optimize the system hardware structure. The cloud data server cluster selects Dell PowerEdge R430 dual-channel rackmount servers with powerful computing capability and scalability, which can meet the needs of large-scale data processing and computing. AS13000 storage system is selected to provide high-capacity, highly reliable storage with data redundancy and backup functions to prevent data loss and ensure data security and fast reading [7]. The switch model is S5130S-28S-EI, which ensures a high-speed and stable network connection and supports the transmission and exchange of large amounts of data. The NGFW4000-UF firewall with a wide coverage domain is selected to guarantee the security of the Cloud Edge Convergence network, preventing external attacks and intrusions, reducing the risk of data loss, and ensuring the stability and efficiency of data transmission. Fig. 2 shows processor architecture.

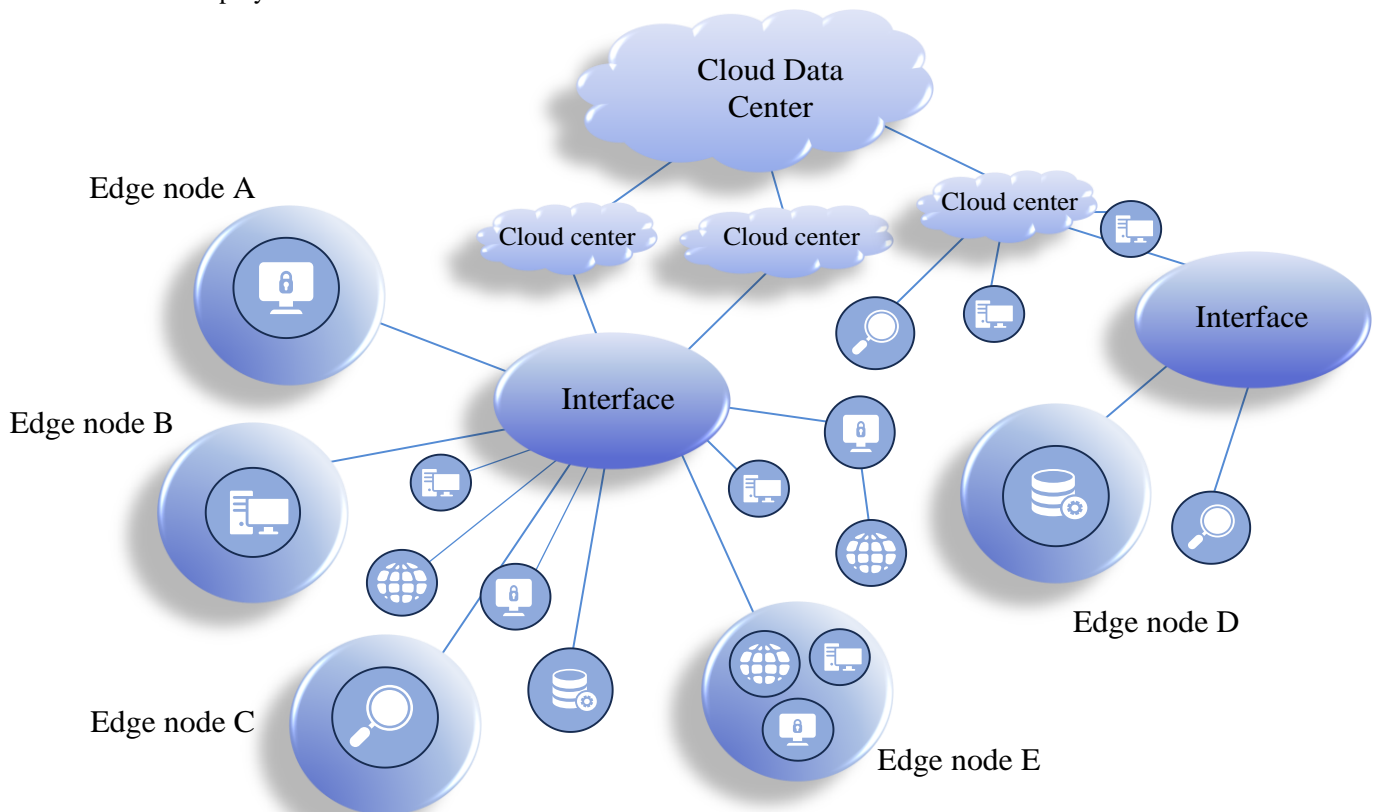


Fig. 1. Cloud edge converged network architecture.

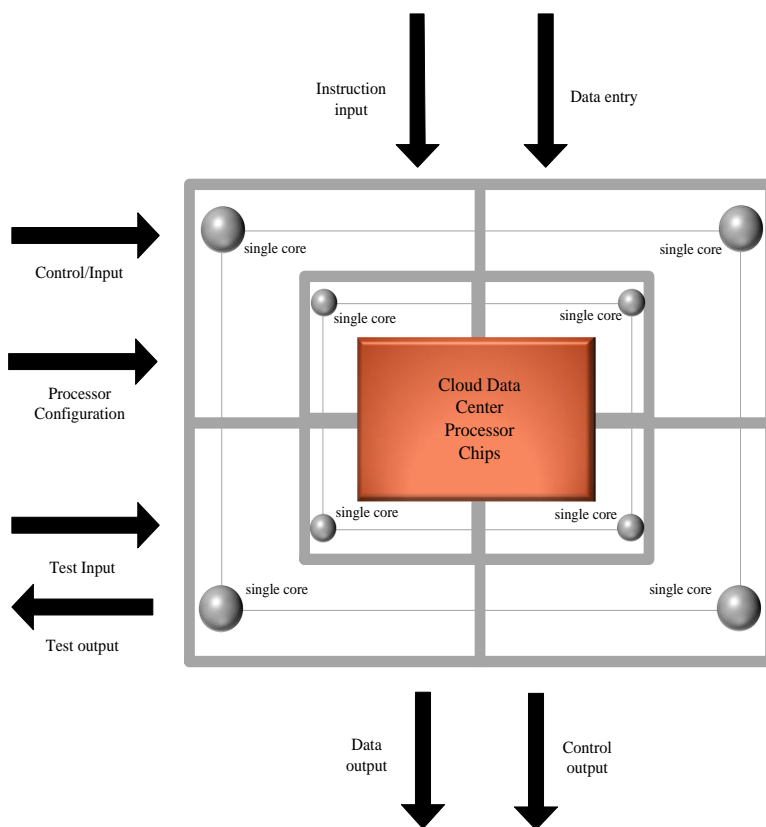


Fig. 2. Processor architecture.

C. Edge Node Structure Optimization

The front-end edge devices mainly include the SICK LMS111 high-precision laser distance sensor, ON Semiconductor MT9V034 high-definition image sensor, DHT11 temperature and humidity sensor, ADXL345 acceleration sensor, which can detect the distance of the transmission and distribution corridor, image, temperature and humidity and motion status [8]. The core terminal equipment of the edge domain is the Lenovo tower server, which is

rugged and suitable for complex environments, and can aggregate massive data in the domain for transmission and pre-processing. Moxa EDS-408A-MM-SC switches provide real-time synchronized edge network connection for the system, which is characterized by high bandwidth and low latency and supports a variety of communication protocols with strong adaptability to guarantee the high efficiency and stability of the edge domain network. Fig. 3 shows edge-core server CPU architecture.

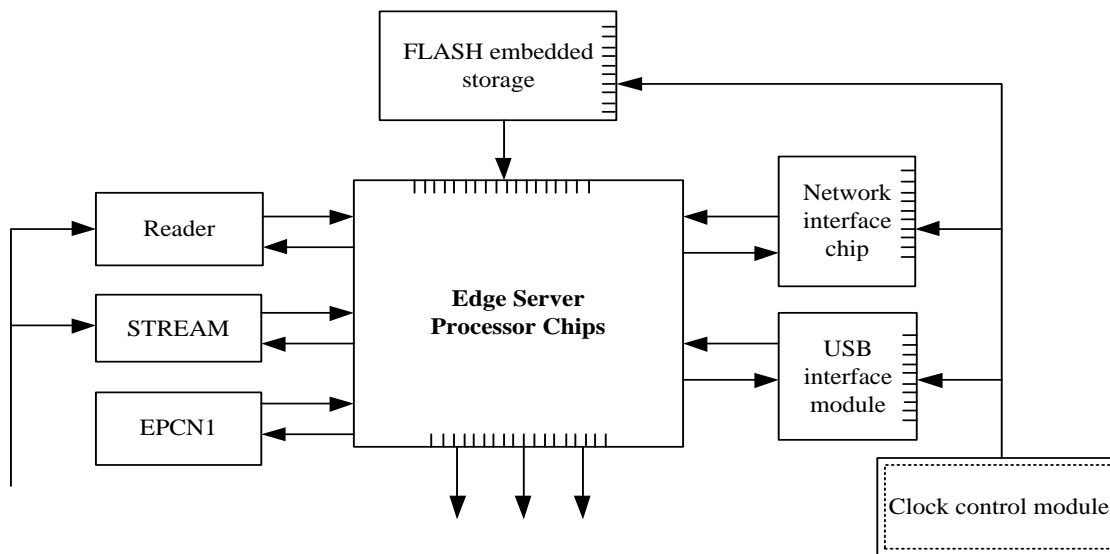


Fig. 3. Edge-Core server CPU architecture.

III. OPTIMIZATION OF IMAGE 3D RECONSTRUCTION TECHNIQUE BASED ON CLOUD EDGE FUSION

A. Non-Sampling Transform Fusion

Aiming at the complex reality of transmission and distribution corridors, non-sampling directional filters are installed at the front end, which can perform filtering operations on signals or images in a specific direction to extract and enhance the signal features in a specific direction while suppressing the interference and noise in other directions, which has important applications in the field of three-dimensional image reconstruction and other fields [9]. Firstly, the image is decomposed at the second level according to the directional component to obtain the quadrant sampling formula:

$$\begin{cases} S_l(i) = 2 * [i / 2] - 2^{l-3} + 1 \\ S^p(i) = 2 * I_0^{p-3} - I_3^{S_l(i)} \end{cases} \quad (1)$$

In the formula, $S_l(i)$ and $S^p(i)$ are the quadrant filter function formulas for random pixel points i in the horizontal and vertical directions, respectively, l is the horizontal quadrant parameter, p is the vertical quadrant parameter, and I is the matrix threshold of the sampling points. The decomposition is performed iteratively for three or more times according to the above steps, and the source image is decomposed into low-frequency sub bands and high-frequency sub bands, which are normalized by wavelet transform. The low-frequency sub band signals are average weighted according to the low-frequency criterion:

$$\begin{cases} P_l = \sqrt{\frac{1}{LP} \sum_L \sum_P [f(i, j) - f(i, j-1)]^2} \\ P_p = \sqrt{\frac{1}{LP} \sum_L \sum_P [f(i, j) - f(i-1, j)]^2} \end{cases} \quad (2)$$

$$P_s = \sqrt{P_l^2 + P_p^2} \quad (3)$$

In the formula, P_l and P_p are the spatial row and column frequencies of the low-frequency sub band averaged and weighted, respectively, and P_s is the low-frequency spatial frequency criterion. The high-frequency sub band signals are regionally energy maximized according to the high-frequency criterion:

$$\begin{cases} E_l(i, j) = \sum_1^{i-1} \sum_1^{j-1} W(i, j) [l(i+L, j+P)]^2 \\ E_p(i, j) = \sum_1^{i-1} \sum_1^{j-1} W(i, j) [p(i+L, j+P)]^2 \end{cases} \quad (4)$$

In the formula, $E_l(i, j)$ and $E_p(i, j)$ are the energy maxima of the high-frequency sub band pixel point (i, j) in the horizontal and vertical regions of space, and W is the regional energy weighting coefficient. The transform fusion is performed by the filtered dual channel, so that the source image is finely preprocessed at the edge end. Fig. 4 shows convolutional neural network workflow visualization.

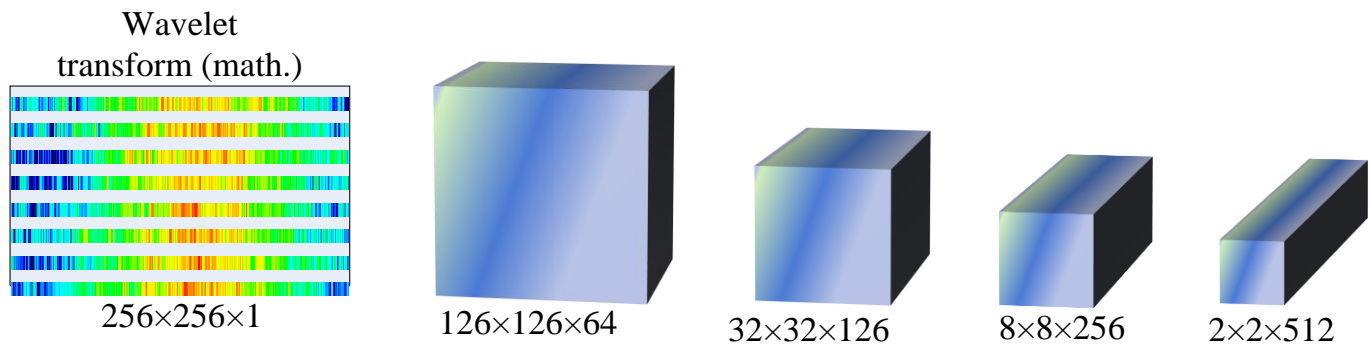


Fig. 4. Convolutional neural network workflow visualization.

B. Edge Detection Constraints

For the source image collected by the infrared laser equipment, there is an edge variability problem, to further guarantee the authenticity of the fused image, the edge information needs to be evaluated constraints. The richness of the image elements is evaluated through the entropy formula:

$$R = \sum_{H=1}^{i=0} P_i \ln P_i \quad (5)$$

In the formula, R represents the entropy value of image

pixel content richness, H is the image resolution grayscale, and P_i is the distribution frequency of pixel point i . The image normalized mean weight δ is introduced for standard deviation calculation to evaluate the image grayscale clarity level:

$$\Delta C = \sqrt{\sum_{L=1}^{i=0} \sum_{P=1}^{j=0} [f(i, j) - \delta]^2 / lp} \quad (6)$$

The larger the standard deviation calculation results,

indicating that the fusion image grayscale dispersion value is higher, the worse the fusion effect, the authenticity and relevance do not meet the standard, need to repeat the above

steps of convolution iterative optimization [10]. Fig. 5 shows grayscale test of edge image.

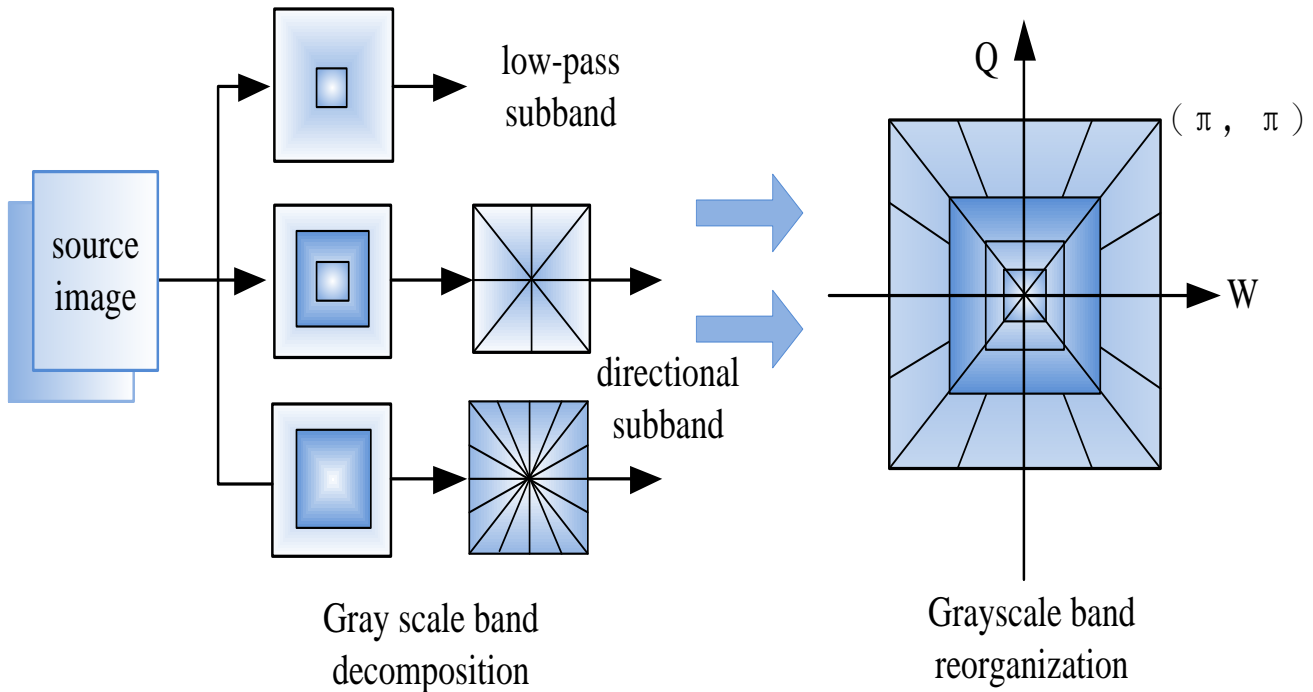


Fig. 5. Grayscale test of edge image.

C. Feature Point Extraction Matching

The preprocessed image information at the edge end is transmitted to the cloud data center for source data archiving in real time via the edge domain network. For the image of the transmission and distribution corridor edge points, line points, corner points, bright spots, dark spots, and other key feature points for localization and extraction, through the Gaussian function convolution to generate three-dimensional scale space:

$$K(x, y, z) = G(x, y, z) \times (x, y) \quad (7)$$

In the formula, $K(x, y, z)$ is the 3D scale space mapping coordinates of the image 2D coordinates (x, y) and $G(x, y, z)$ is the Gaussian function convolution coordinate parameter. The Gaussian difference is utilized to detect the three-dimensional spatial coordinate point poles:

$$J(x, y, z) = (G(x, y, z\beta) - G(x, y, z)) * (x, y) \quad (8)$$

According to the calculation results, the three-dimensional spatial discrete extreme points are extracted, and then the feature points are localized by three-dimensional quadratic function fitting to eliminate the edge points with poor stability [11]. Due to the existence of dynamics in the real-time monitoring of cloud edge fusion, the gradient method is used to carry out a balanced and stable simulation of the moving

structure of the feature points in a specific direction, and the description of the baseline feature direction is obtained as:

$$D(x, y) = \sqrt{(K(x+1, y) - K(x-1, y))^2 + (K(x, y+1) - K(x, y-1))^2} \quad (9)$$

$$Dir(x, y) = \tan^{-1} \left(\frac{K(x, y+1) - K(x, y-1)}{K(x+1, y) - K(x-1, y)} \right) \quad (10)$$

In the formula, $D(x, y)$ denotes the gradient value of the feature point and $Dir(x, y)$ denotes the spatial reference direction of the feature point. The feature points are extracted from the 3D reconstructed spatial point cloud to generate a descriptor. The descriptor contains the local geometric information of the feature point, and the SIFT (Scale Invariant Feature Transform) algorithm is used to generate the feature point description vector:

$$M(x_i, y_i) = Dir(x, y) * \Delta T(x_i + y_i) \quad (11)$$

In the formula, $M(x_i, y_i)$ is the dynamic scale description vector in the reference direction and ΔT is the 3D coordinate mapping dynamic time difference. Based on the description vector, dynamic image 3D point cloud reconstruction can be performed, which utilizes the camera position and point cloud information to project each pixel point of the image into the 3D space [12].

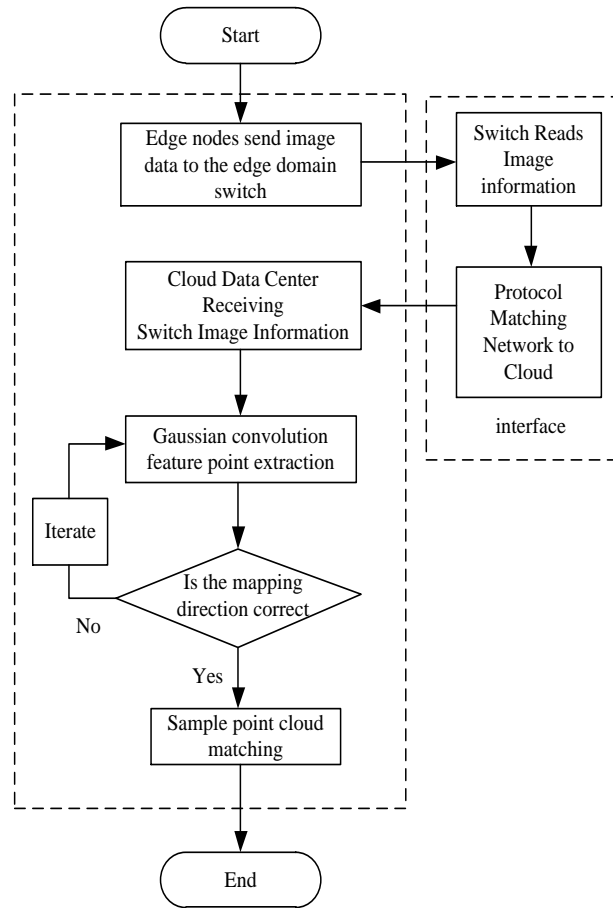


Fig. 6. Cloud edge collaborative feature point extraction process.

D. Point Cloud Synchronized 3D Reconstruction

Based on the basic geometric structure and moving position described by the feature point vectors, the key feature points with high edge dispersion are extracted to construct a sparse point cloud for localization and reconstruction in 3D space [13]. However, the sparse only contains a small number of salient feature points, which cannot accurately describe the 3D details of the transmission and distribution corridor, and further dense point cloud reconstruction is required [14]. First, the data collected by the edge devices are synchronously transmitted to the cloud data center, and the sparse point cloud is arranged from near to far according to the camera positional distance to obtain the feature-matching initialization sequence:

$$A(w) = \left\{ w_i \mid w_i \in w_m, n(w) \cdot \frac{O(w)O(w_i)}{|O(w)O(w_i)|} > \cos \alpha \right\} \quad (12)$$

In the formula, $A(w)$ is the set of sequence images, w_i denotes the image i , $O(w)$ is the center point of the surface of the fused image, $O(w_i)$ is the center of the focused light of the camera of the fused image, and α is the maximum value of the angle between the largest edge point within the image and the center of the camera. Face sheet expansion is performed on the neighboring images in the sequence:

$$Q(w) = \{ Q_i(x', y') \mid w \in Q_i(x, y), |x - x'| + |y - y'| = 1 \} \quad (13)$$

In the formula, (x, y) and (x', y') are the corresponding point clouds of neighboring image facets. To ensure the authenticity of the extended image, the facets with anomalies in the extended fusion are filtered, and the neighboring image facets are screened by the consistency test:

$$|Q'(w)|(1 - hid^*(w)) < \sum_{w_i \in W(w)} 1 - hid^*(w) \quad (14)$$

In the formula, $hid^*(w)$ is the grayscale consistency test function. If the tested image facets satisfy the above conditions, it means that the two image facets have large differences and are not suitable for extended reconstruction. Based on the consistency fusion test, the dense point cloud can accurately capture the key geometric structures in the corridor, and the processed dense point cloud data is converted into a 3D mesh model using the Power Crust algorithm [15]. Fig. 6 shows cloud edge collaborative feature point extraction process.

A set of discrete extreme values highlighted in the image is extracted as the simulation center axis, the point cloud is linearly estimated and regionally divided, adjacent points are connected to generate a Voronoi diagram, the extreme points

of each cell Voronoi diagram are extracted, i.e., the feature points of each region that are farthest away from the sampling points, and the weighted computation is performed to get the description of the reconstruction of the three-dimensional Power diagram [16]:

$$U_{pow(x,\varphi_{o,u})} = U^2(o, x) - \eta^2 \quad (15)$$

In the formula, $U_{pow(x,\varphi_{o,u})}$ is the weighted stereo Power map distance description of the extreme point, U is the

distance of the extreme point from the sampling center, $\varphi_{o,u}$ represents a sphere with O as the center and a radius of u , and η^2 is the reconstruction weighting value. Each region of the image features a point cloud in turn for three-dimensional reconstruction, to get the three-dimensional framework, comprehensively improve the image's three-dimensional reconstruction accuracy (see Fig. 7). The texture information in the original image is extracted and mapped onto the surface of the 3D model, which makes the transmission and distribution corridor model more realistic and vivid and can effectively enhance the realism of the digital model [17].

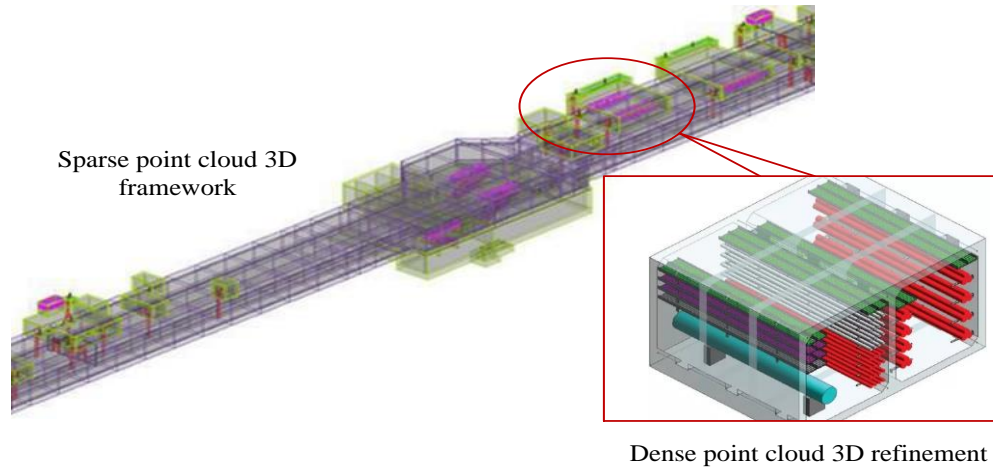


Fig. 7. 3D reconstructed view of point cloud.

IV. SYNCHRONIZED UPDATE OF 3D RECONSTRUCTION DATA FOR CLOUD EDGE COLLABORATIVE IMAGES

A. Dynamic Estimation of Feature Points

The transmission and distribution corridor monitoring equipment is subjected to remote manipulation for displacement, and the images need to be evaluated for feature point motion. Assuming that the equipment moves at the same speed as the pre-set parameters, the dynamic estimation model is expressed as:

$$\begin{bmatrix} v_{\gamma 1} \\ v_{\gamma 2} \\ v_{\gamma 3} \\ v_{\gamma 4} \end{bmatrix} = \frac{1}{r} \begin{bmatrix} 1 & 1 & long_n \\ -1 & 1 & -long_n \\ -1 & 1 & long_n \\ 1 & 1 & -long_n \end{bmatrix} \begin{bmatrix} v_x \\ v_y \\ v_z \end{bmatrix} \quad (16)$$

In the formula, v_{γ} represents the angular velocity parameter of the device moving different gears, $long_n$ is the distance of the device running for one week, v_x and v_y are the moving speeds of the device in the x and y directions, and r is the radius of the McNamee wheel [18].

The time difference variable Δt of the dynamic image facets is calculated to recognize the dynamic position of the sequence image feature points, and the displacement coordinate variable is extracted to be fused with the 3D

reconstruction data:

$$dt_{ni} = LinarInterp\left((x_i, y_i), \frac{long_{ni+1} - long_{ni}}{\Delta t}\right) \quad (17)$$

Through dynamic estimation, the synchronized transmitted images can be analyzed and compared in a more detailed way, and the optimal data can be selected for fusion and three-dimensional reconstruction to reduce the distortion of information due to light and shadow and noise in the moving process.

B. Incremental Learning Synchronization Update

After the initial reconstruction of the 3D image, continuous optimization of the 3D reconstructed data is achieved by incremental learning allowing the 3D model to continuously learn from and update new data while retaining knowledge of the existing data [19]. The edge network transmits new image or scan data to the cloud data center and continuously adds new image frames using the Incremental SFM (Structure for Recovery of Motion) algorithm to 3D map the real-time data onto the existing 3D knowledge [20]:

$$\tilde{R}(x, y, z | \Delta t) = \sum_{N'}^{i=1} y_n \log \frac{\exp(o_i)}{\sum_{N'} \exp(o_i)} \quad (18)$$

In the formula, $\tilde{R}(x, y, z | \Delta t)$ represents the cross entropy of 3D reconstructed feature points under uniform

synchronization conditions, $\exp(o_i)$ and $\exp(o_i)$ represent the original feature point center position and the incremented feature point center position, respectively. The dynamic synchronization data is introduced to iterate the network weights λ to calculate the extra data loss existing in the synchronization process:

$$loss(\tilde{R}^t) = \frac{1}{2} \sum_{|\tilde{R}^{t-1}|}^{i=1} \lambda (\tilde{R}_i^{t-1} - \tilde{R}_i^t)^2 \quad (19)$$

It solves the problem of data synchronization inconsistency in 3D reconstruction through incremental learning, and supports long-time continuous learning and optimization to eliminate image data discrepancies and improve the consistency and accuracy of large-scale image 3D reconstruction (see Fig. 8).

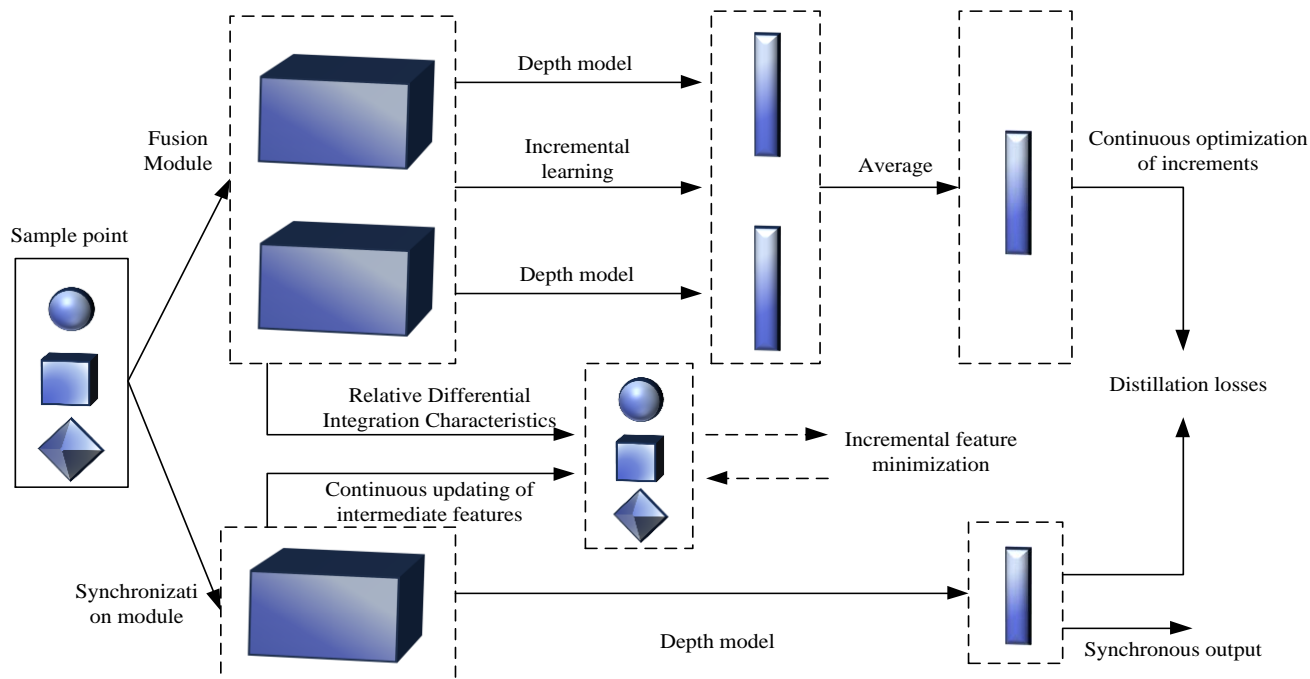


Fig. 8. Incremental learning synchronization mechanism.

V. EXPERIMENTAL RESEARCH

To verify the application effectiveness of large-scale image 3D reconstruction technology based on cloud edge fusion architecture and the optimized performance of cloud edge data synchronous update technology, a comparison experiment is designed for image acquisition and 3D reconstruction of transmission and distribution corridors. The experimental cloud data center equipment is selected from Dell Power Edge R430 dual-channel rack servers, and the edge core equipment is selected from Lenovo tower servers, with a unified setup of 8Mbps upstream broadband, and the collected images of transmission and distribution corridors are visualized using MATLAB software, to carry out comprehensive technical evaluation of the network latency state, matching performance, and reconstruction time of the large-scale image three-dimensional reconstruction method. A comprehensive technical evaluation is carried out.

A. Synchronization Update Network Latency Evaluation

The changing dynamics of the synchronization update network state of the image transmission from the front-end device to the system host computer is shown in Fig. 9.

According to the above figure, it can be seen that the data throughput of the cloud edge network based on cloud edge fusion technology is larger, the average throughput is always above 20000 Kbps, and the highest throughput can reach 42000 Kbps. The centralized cloud communication technology used for tilt photography has an average network throughput of about 10000 Kbps to 20000 Kbps due to the lack of a two-end synergistic mechanism. The larger the network throughput, the faster the synchronization and updating speed for large-scale images, so the image synchronization transmission delay time of the cloud-side cooperative network is the shortest, with a maximum of no more than 85 ms and a minimum of only 19 ms, which is significantly better than the other two methods in terms of synchronization transmission speed.

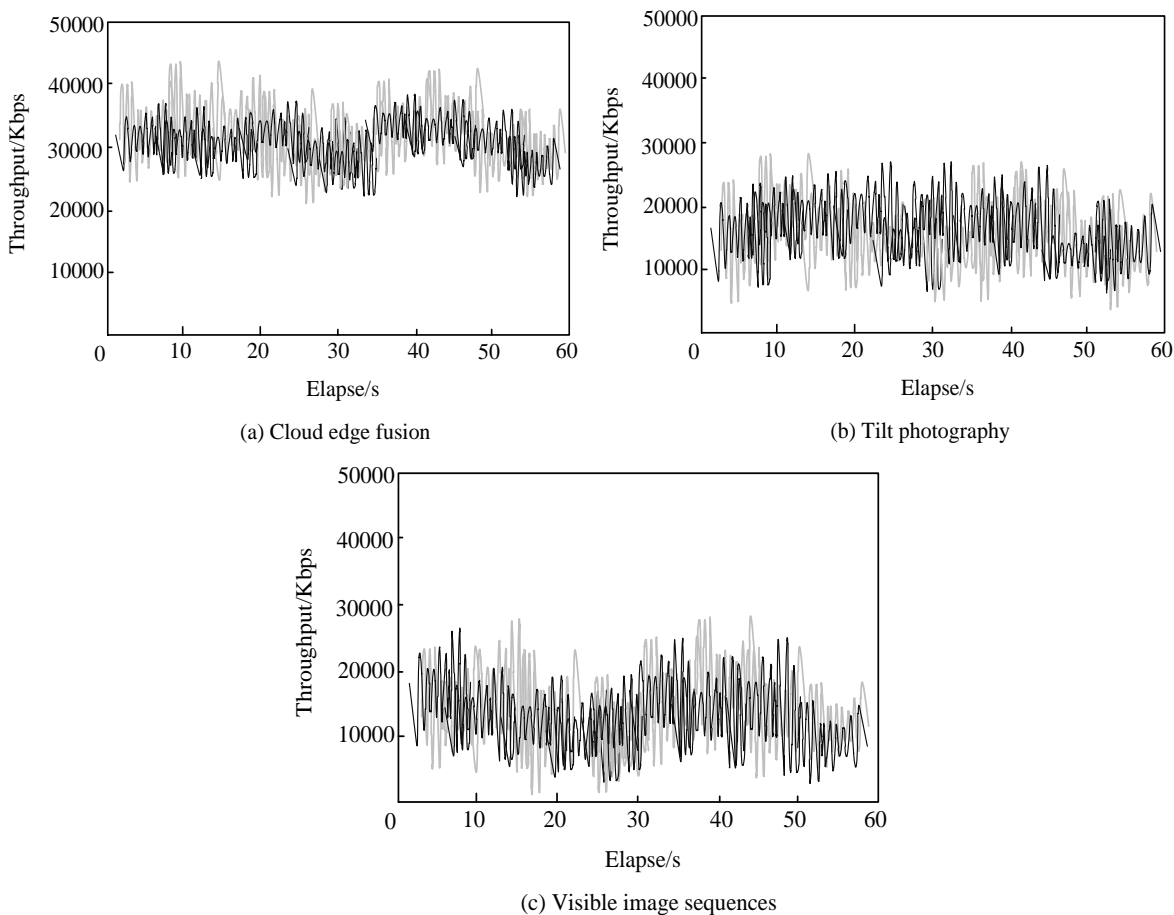


Fig. 9. Network communication throughput.

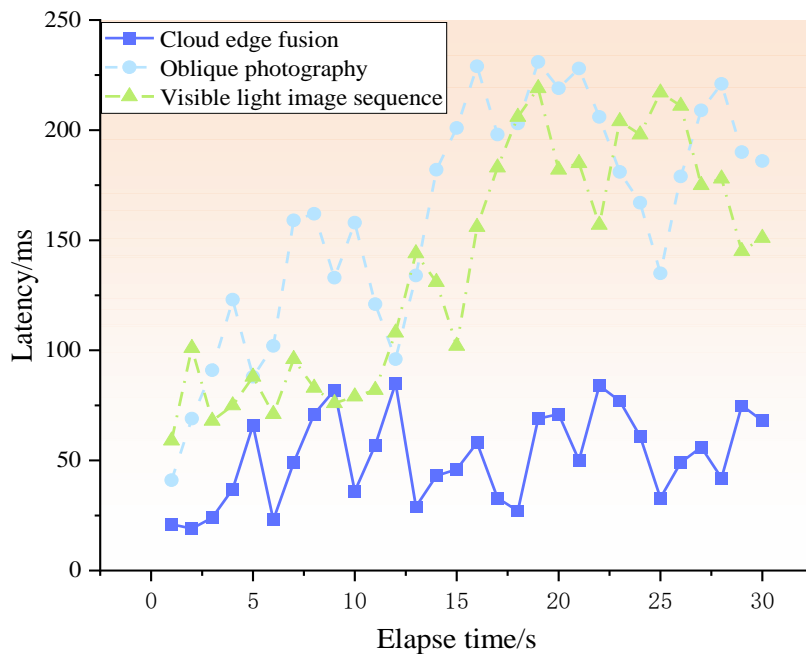


Fig. 10. Network synchronization delay.

B. Image 3D Reconstruction Time Evaluation

To check the processing time of large-scale image 3D reconstruction stages, 50, 100, 200, and 300 images are fused

and reconstructed respectively, and the time required for each stage is statistically shown below.

TABLE I. STATISTICS OF 3D RECONSTRUCTION DURATION FOR CLOUD-EDGE FUSION

Number of images	Duration of the first phase(min:s)	Point cloud upload time(min:s)	Duration of the second phase (min:s)	Total processing time (min:s)
50	01:48	02:15	03:23	07:26
100	03:21	03:46	06:58	14:05
200	10:17	07:31	09:18	27:06
300	21:39	17:28	19:42	58:49

TABLE II. STATISTICS ON THE DURATION OF 3D RECONSTRUCTION FOR TILT PHOTOGRAPHY

Number of images	Duration of the first phase (min:s)	Point cloud upload time (h:min:s)	Duration of the second phase (min:s)	Total processing time (h:min:s)
50	06:28	04:10	04:33	15:11
100	11:45	25:26	07:12	44:23
200	25:59	1:09:41	21:37	1:57:17
300	40:27	1:25:58	31:02	2:37:27

TABLE III. STATISTICS OF 3D RECONSTRUCTION DURATION OF THE VISIBLE IMAGE SEQUENCE

Number of images	Duration of the first phase (min:s)	Point cloud upload time (h:min:s)	Duration of the second phase (min:s)	Total processing time (h:min:s)
50	07:18	12:15	06:23	25:55
100	15:21	35:33	13:08	64:02
200	31:37	1:17:21	24:14	2:13:11
300	56:32	1:37:05	39:42	3:33:19

The data in Tables I to III show that cloud-edge fusion uses a cloud-edge cooperative network with a higher synchronization rate, and the time taken in the image point cloud upload phase is much lower than that of the tilt photography and visible sequence techniques. When the number of fused reconstructed images is 300, the first stage of image feature extraction and preprocessing of cloud edge fusion takes 21:39 min, point cloud uploading takes 17:28 min, and the second stage of point cloud reconstruction takes 19:42 min. The total processing time of the whole stage of 3D reconstruction of cloud edge fusion is only 58:49 min, whereas tilt photography requires a total time of 2:37:49 min. The total processing time

for the whole phase of 3D reconstruction is only 58:49 min, while the total time required for tilt photography is 2:37:27 h, and the total time used for the visible light sequence is 3:33:19 h. Thus, it can be seen that the cloud-edge fusion technology not only has good network synchronization performance but also has obvious advantages in image feature extraction and point cloud reconstruction functions.

C. Reconstruction Matching Performance Evaluation

It is verified that the cloud-edge fusion 3D reconstruction technique has good network synchronization performance, and further evaluation of its matching performance is still needed.

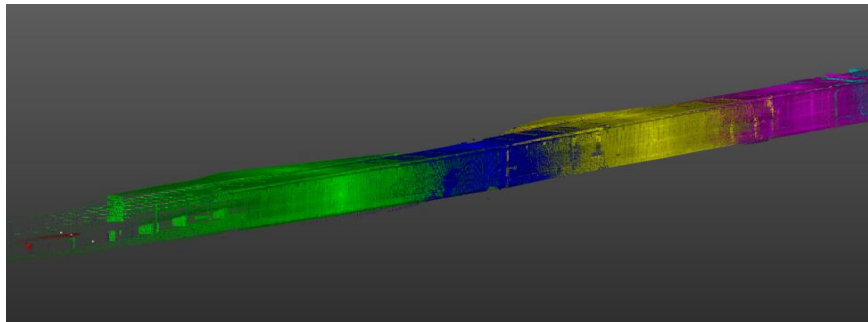


Fig. 11. 3D reconstruction of the visualized image.

Completing the 3D reconstruction of the transmission and distribution digital corridor, the statistics of the number of matches, the number of matching points, the success rate of

matching, and the length of time taken for the three methods of identification are shown in the following Table IV.

TABLE IV. COMPARISON OF THREE-DIMENSIONAL RECONSTRUCTION MATCHING PERFORMANCE

Methodologies	Number of matches/times	Match Points/Each	Match rate/%	Timing
Cloud Edge Fusion	5981	3925	96.72	1 h 11 min
Oblique photography	25883	1098	80.35	3 h 05 min
Visible Image Sequence	30768	875	72.64	3 h 58 min

According to the data in Table IV, it can be seen that for 3D reconstruction of the same transmission and distribution corridor image, the cloud-edge fusion technique takes the shortest time and carries out the least number of matches, but successfully recognizes and matches the greatest number of point clouds, with a total of 3925 matching points identified, and the matching success rate is as high as 96.72%. In summary, the cloud-edge fusion 3D reconstruction technique has efficient synchronization efficiency of the cooperative network and also has a good application effect in the point cloud recognition and matching function, which has significant advantages over other methods.

VI. DISCUSSION

The research results show that the synchronous update and optimization method for large-scale image 3D reconstruction technology based on cloud-edge fusion architecture has significant application advantages. On the one hand, the architecture can efficiently integrate cloud and edge computing resources, dynamically allocate them according to the task demand, hand over the computationally intensive work to the cloud, and the edge end is responsible for data acquisition and pre-processing, which greatly improves the resource utilization rate. On the other hand, the edge end can perform local preliminary processing of image data, reducing the time delay of transmission to the cloud. The synchronous update mechanism gives the technology adaptability and flexibility to adapt to changing image data and application scenarios, and the cloud-edge convergence architecture can be flexibly expanded and deployed according to actual needs to meet the needs of different scales and types of applications.

The author believes that the technology has great potential for development and has a bright future. In the future, it can further explore smarter resource allocation strategies and synchronized update mechanisms, improve the degree of system automation and efficiency, and achieve more innovative breakthroughs by combining advanced technologies such as artificial intelligence and 5G communication. In addition, research on data security and privacy protection should be strengthened to ensure the safe storage and transmission of large-scale image data under the cloud-side convergence architecture, so as to bring more efficient, accurate, and reliable image 3D reconstruction solutions to many fields.

VII. CONCLUSION

Aiming at the problem of three-dimensional reconstruction of power transmission and distribution corridors, this paper optimizes the design of large-scale image three-dimensional

reconstruction technology and its synchronous update performance under the cloud-edge fusion architecture, and mainly completes the following research: Establish the transmission and distribution digital corridor IoT cloud-edge fusion network architecture, optimize the cloud data center and edge node structure; Optimize the accuracy of cloud-edge fusion 3D reconstruction point cloud matching by using non-sampling filtering, edge checking, and Gaussian convolution; Enhance the synchronous updating performance of cloud-edge cooperative networks through dynamic evaluation of feature points and incremental learning algorithm.

It can be seen through experiments that the cloud-edge fusion 3D reconstruction technology can realize accurate image 3D reconstruction in a short time, the information synchronization update delay rate is low, and the processing time is shorter. Although the results of this paper have the above advantages, there are still some shortcomings: Cloud edge fusion technology requires higher compatibility equipment configuration, higher application costs, and relatively greater technical difficulties; 3D reconstruction software for image fusion detail processing and model training balance control is insufficient, there are still errors and distortion. Future research needs to be deepened from the above perspectives to comprehensively improve the efficiency and accuracy of the application of cloud edge fusion 3D reconstruction systems.

REFERENCES

- [1] Feng Xiao; Li Bingran; Bai Chenxu. Three-dimensional reconstruction of transmission line based on oblique photogrammetry. *Electrotechnical Application*, 2020, 39(3):51-54.
- [2] Zhang Lu, Yuan Wei, Liu Xiaolin. Research on Three-dimensional Reconstruction Model of Transmission Line Corridors based on Visible Light Image Sequences. *Electric Power Equipment Management*, 2023(11):96-98.
- [3] Song Yaqin; Xu Hui; Liu Xianfeng; Wang Yapeng; Cheng Zhimi; Wang Hucheng; Chen Shanzhi. Cloud-Edge Collaboration Architecture and Key Technologies for 6G Integrated Satellite and Terrestrial Network. *Space-Integrated-Ground Information Networks*, 2023, 4(3):3-11.
- [4] Yang Hang; Chen Rui; An Shipeng; Wei Hao; Zhang Heng. The growth of image-related three dimensional reconstruction techniques in deep learning-driven era: a critical summary. *Journal of Image and Graphics*, 2023, 28(8):2396-2409.
- [5] Zhang Lei; Shi Yan; Lu Wenyong; Xu Rui; Jin Zhan; Luo Weijie; Cehn Yi; Zhao Chunliu; Zhan Chunlian. 3D reconstruction technique based on SURF-OKG feature matching. *Optics and Precision Engineering*, 2024, 32(6):915-929.
- [6] Su Yu; Zhang Zexu; Yuan Mengmeng; Xu Tianlai; Deng Hanzhi; Wang Jing. A Point Cloud Fusion Method for Space Target 3D Laser Point Cloud and Visible Light Image Reconstruction Method. *Journal of Deep Space Exploration*, 2021, 8(5):534-540.

- [7] Ren Mengxin, Yang Jianfeng, Deng Zhougray, Zou Qiong, Tong Tianle. 3D Reconstruction Method Based on PP-Matting and Incremental Structure-from-Motion. *Modeling and Simulation*, 2023, 12(4):4116-4126.
- [8] Zhou X, Xu X, Liang W, et al. Deep-Learning-Enhanced Multitarget Detection for End-Edge-Cloud Surveillance in Smart IoT. *IEEE internet of things journal*, 2021(8-16):12588-12596.
- [9] Zhang E, Hu K, Xia M, et al. Multilevel feature context semantic fusion network for cloud and cloud shadow segmentation. *Journal of Applied Remote Sensing*, 2022, 16(4):1-26.
- [10] Shang X. Enabling Data-intensive Workflows in Heterogeneous Edge-cloud Networks. *Performance Evaluation Review*, 2022,50(03):36-38.
- [11] Jiang S, Gao H, Wang X, et al. Deep reinforcement learning based multi-level dynamic reconfiguration for urban distribution network: a cloud-edge collaboration architecture. *Global Energy Interconnection*, 2023, 6(1):1-14.
- [12] Wang Z, Ko I Y. Edge-Cloud Collaboration Architecture for Efficient Web-Based Cognitive Services. *2023 IEEE International Conference on Big Data and Smart Computing (BigComp)*, 2023:124-131.
- [13] Wang M, Liu R, Yang J, et al. Traffic Sign Three-Dimensional Reconstruction Based on Point Clouds and Panoramic Images. *Photogrammetric record*, 2022(Mar. TN.177):37.
- [14] Gaige D, Rongwu W, Chengzu Li, et al. Three-Dimensional Model Reconstruction of Nonwovens from Multi-Focus Images. *Journal of Donghua University (English version)*, 2022(003):185-192.
- [15] Iacoviello P, Bacigaluppi S, Gramegna M, et al. Microsurgical Three-Dimensional Reconstruction of Complex Nasal and Midfacial Defect: Multistep Procedure Respecting Aesthetic Unit Criteria. *Journal of Craniofacial Surgery*, 2021,(32):1517-1520.
- [16] Shan C, Yao Q, Cao S, et al. Measurement of fracture development evolution of coal samples under acid-alkaline by three-dimensional reconstruction and AE time-frequency characteristic analysis. *Measurement*, 2023(217):1-23.
- [17] Zhang C, Guo Y, Meng D, et al. Hybrid iteration and optimization-based three-dimensional reconstruction for space non-cooperative targets with monocular vision and sparse lidar fusion. *Aerospace Science and Technology*, 2023(140):1-16.
- [18] Zhao L, Pan J, Xu L. Cone-Beam Computed Tomography Image Features under Intelligent Three-Dimensional Reconstruction Algorithm in the Evaluation of Intraoperative and Postoperative Curative Effect of Dental Pulp Disease Using Root Canal Therapy. *Scientific programming*, 2022(3):1-8.
- [19] Zhao M, Lin M, Xu P. A Study on the Whole-skin Peeling System of a Snakehead Based on Three-dimensional Reconstruction. *Applied Engineering in Agriculture*, 2022(38):741-751.
- [20] Zhang F, Pan H, Zhang X, et al. Three-dimensional reconstruction for flame chemiluminescence field using a calibration enhanced non-negative algebraic reconstruction technique. *Optics Communications: A Journal Devoted to the Rapid Publication of Short Contributions in the Field of Optics and Interaction of Light with Matter*, 2022(520):1-10.